Communications in Mathematics and Applications
Vol. 14, No. 2, pp. 727–744, 2023
ISSN 0975-8607 (online); 0976-5905 (print)
Published by RGN Publications
DOI: 10.26713/cma.v14i2.2169

http://www.rgnpublications.com

Research Article

Driver Predictions and Energy Consumption in Car-following Model with BFL Effect

Sunita, Meenakshi and Poonam Redhu*

Department of Mathematics, Maharshi Dayanand University, Rohtak 124001, Haryana, India
***Corresponding author:** poonamr.maths@mdurohtak.ac.in

Received: January 11, 2023 **Accepted:** May 30, 2023

Abstract. In real life, there is a significant role of neighboring vehicles as well as driver's behavior in the nonlinear dynamics of traffic flow. Based on the car-following model, we examined the impact of individual expectations on a single-lane highway with a *Backward-Forward Looking* (BFL) effect on traffic flow. The model's stability criterion is determined through linear and nonlinear analysis, and it is observed that the prediction parameter not only reduces the unstable region but is also helpful in reducing energy consumption. Moreover, it is also remarked that the driver's prediction effect will become more effective in the case BFL model. Furthermore, the numerical simulation demonstrates that the new model effectively enhances stable regions and it should be considered during the modeling of traffic flow.

Keywords. Energy consumption, Car-following model, Backward looking effect, Individual expectation

Mathematics Subject Classification (2020). 00A05, 00A69, 00A79

1. Introduction

Traffic congestion has emerged as one of the major social and economic issues relating to transportation in developed nations as a result of the expansion of urbanisation and motorization. Today's traffic congestion is increasingly complicated and is creating environmental pollution, noise pollution, energy waste, and other problems due to the quick growth of automobiles and the worldwide economy. Understanding traffic flow operations is essential for managing these issues and reducing congestion. Various mathematical models,

including macroscopic [3, 18, 20, 23, 29, 36], microscopic [4, 6, 12, 25, 35, 43] and mesoscopic [5, 13, 39] have been studied in this direction.

One of them is the car-following model which comes under the category of a microscopic approach that is used to characterize individual vehicles and driver's behavior. Among the car-following models, the optimal velocity model [2] has auspiciously disclosed the gradual development of traffic congestion in an easy way. Numerous modified models [8, 11, 16, 34, 41] have been developed with the effects of various traffic components and these extended models were successfully able to illustrate the nature of traffic congestion in a more precise way upto some extent.

As we know the neighboring vehicles significantly affect the traffic flow. To illustrate the real traffic situation, some investigations on the influence of backward-looking have been conducted in recent year [7, 14, 21, 22, 32, 33, 40], as the majority of car-following models focused on the forwarding vehicle. By introducing the effect of backward-looking, Sun *et al.* [32] proposed the *Backward Looking Velocity Difference* (BLVD) model in which the driver assumed the car's rear-view mirror to monitor the situation of the back vehicle in order to ensure safe driving.

As many complex aspects influence real-time traffic, including pedestrians, competency, driver attention, and so on and such external influences are represented as disturbances in the uniform flow leading to changes in operating speed. In comparison to the situation of no disturbance, these variations in speed result in increased energy consumption [24]. Wei and Yu [37] investigated the relationship between traffic flow stability and energy consumption estimated by many common car-following models and discovered that reducing energy usage is dependent on traffic flow stability. Also, sudden deceleration and acceleration may waste a lot of energy in various traffic scenarios [17, 19, 31].

In real-world traffic, drivers frequently anticipate their speed based on the traffic conditions [10, 26, 28, 30]. In this direction, Zheng *et al.* [42] demonstrated an anticipatory driving model based on FVD model. Peng and Cheng [27] included the expectation optimal velocity in the driver's behavior to investigate the consequences of the anticipation optimal speed. Yi-Rong *et al.* [38] estimated the reaction delay and predict behavior of the driver in the car-following model which has a significant impact on whether the traffic system is stable or not. Also, Jafaripournimchahi *et al.* [15] examined the impact of driver memory with the anticipation effect on traffic flow. However, to achieve a more effective description of traffic congestion, we investigate the impact of driver's prediction effect under the environment of backward-forward-looking and analyze how these factors affect traffic flow stability and energy consumption at the same time in our proposed model.

The following is a description of the paper's structure. In Section 2, we review the basic models and introduce a new car-following model. Linear and nonlinear stability are examined in Sections 3 and 4, respectively. Section 5 carried out numerical simulation, furthermore, energy consumption is a widely discussed issue, and we seek to identify the energy consumption in Section 6 and finally, in Section 7, there is a conclusion.

2. Model Formulation

To characterize car-following behavior on a one-lane road, Bando *et al.* [1] developed the *Optimal Velocity* (OV) model. The model equation is

$$\frac{dv_k(\widetilde{t})}{d\widetilde{t}} = \widetilde{a}[V(\Delta x_k(\widetilde{t})) - v_k(\widetilde{t})]. \tag{2.1}$$

Here $x_k(\widetilde{t})$ and $v_k(\widetilde{t})$ are the position and velocity of car k at time $\widetilde{t}$, $\Delta x_k(\widetilde{t}) = x_{k+1}(\widetilde{t}) - x_k(\widetilde{t})$ shows the distance travelled by two vehicles in succession, $\widetilde{a}\left(=\frac{1}{\tau}\right)$ is the sensitivity of a driver, and $V(\Delta x_k(\widetilde{t}))$ is the optimal velocity function. In the above model, high acceleration and unreasonable deceleration appeared. To resolve these problems, Jiang *et al.* [16] proposed the *Full Velocity Difference* (FVD) model by adding the positive relative velocity. The dynamical equation is

$$\frac{dv_k(\widetilde{t})}{d\widetilde{t}} = \widetilde{a}[V(\Delta x_k(\widetilde{t})) - v_k(\widetilde{t})] + \lambda \Delta v_k(\widetilde{t}), \tag{2.2}$$

where λ is coefficient of velocity difference, $\Delta v_k(\widetilde{t}) = v_{k+1}(\widetilde{t}) - v_k(\widetilde{t})$ represents the difference in velocity between the following car $k+1$ and the pursing car k. To study the effect of preceding vehicles, Hossain *et al.* [14] presented the improved car-following model considering modified velocity difference and backward optimal velocity as

$$\frac{dv_k(\widetilde{t})}{d\widetilde{t}} = \widetilde{a}[\omega V_F(\Delta x_k(\widetilde{t})) + (1-\omega)V_B(\Delta x_{(k-1)}(\widetilde{t})) - v_k(\widetilde{t})] + \lambda \Delta v_k(\widetilde{t}), \tag{2.3}$$

where ω is the forward driver weight parameter and $(1-\omega)$ represents the backward driver weight parameter. The optimal velocity functions are $V_F(\Delta x_k(\widetilde{t}))$ and $V_B(\Delta x_k(\widetilde{t}))$ for forward and backward observations, respectively. It is found that the region of stability enhances by considering the role of preceding vehicles.

In order to investigate the delay due to driver or vehicle, Peng and Cheng [27] observed that the anticipation parameter in optimal velocity has a substantial impact on traffic flow and proposed a model named as *Anticipation Optimal Velocity Model* (AOVM), with the model equation is given as

$$\frac{dv_k(\widetilde{t})}{d\widetilde{t}} = \widetilde{a}[V(\Delta x_k(\widetilde{t}+\alpha\tau)) - v_k(\widetilde{t})] + \lambda \Delta v_k(\widetilde{t}), \tag{2.4}$$

where $\alpha \geq 0$ denotes the prediction effect, $V(\Delta x_k(\widetilde{t}+\alpha\tau))$ is the expected optimal velocity, which means the expected optimal speed is adjusted by the driver at time $\widetilde{t}+\alpha\tau$.

The previously-mentioned models can explain some complex traffic patterns (e.g. congestion and instability in traffic flow). To keep away from the rear-end collision and maintain safe driving, in effective traffic flow, the driver should use the rear-view mirror to simultaneously detect the running conditions of the car in the rear. In addition, based on the current traffic scenario, the driver frequently calibrates his velocity after a time delay and evaluates his individual driving behavior. Therefore, we presented a novel car-following model that takes into account the driver's predictive behavior as well as the BFL effect. The proposed model is

$$\frac{dv_k(\widetilde{t})}{d\widetilde{t}} = \widetilde{a}[\omega V_F(\Delta x_k(\widetilde{t}+\alpha\tau)) + (1-\omega)V_B(\Delta x_{k-1}(\widetilde{t}+\alpha\tau)) - v_k(\widetilde{t})] + \lambda \Delta v_k(\widetilde{t}+\alpha\tau), \tag{2.5}$$

where $\Delta x_k(\widetilde{t}+\alpha\tau)$ and $\Delta v_k(\widetilde{t}+\alpha\tau)$ is the driver's prediction information of the difference in position and velocity between the following car $k+1$ and the pursuing car k at time $\widetilde{t}+\alpha\tau$, respectively.

Depending on the sign of the prediction coefficient α, the new model can explain two different aspects of the driver's individual expectation behavior during motion. Firstly, $\alpha > 0$ stands for the driver's predicted effect in driving behavior, and secondly, $\alpha < 0$ corresponds to the response lag tendency of drivers. In actual traffic, the driver generally requires time to feel and respond to the stimuli of the road, for instance, relative velocity, and variation of headway, and then make a decision to adjust the acceleration of their vehicle.

Expanding eq. (2.5) by using the Taylor expansion of the variables $\Delta x_k(\widetilde{t}+\alpha\tau)$ and $\Delta v_k(\widetilde{t}+\alpha\tau)$ while ignoring the nonlinear terms, result in the equation as given below:

$$\Delta x_k(\widetilde{t}+\alpha\tau) = \Delta x_k(\widetilde{t}) + \alpha\tau\Delta x_k'(\widetilde{t}) = \Delta x_k(\widetilde{t}) + \alpha\tau\Delta v_k(\widetilde{t}), \tag{2.6}$$

$$\Delta x_{k-1}(\widetilde{t}+\alpha\tau) = \Delta x_{k-1}(\widetilde{t}) + \alpha\tau\Delta x_{k-1}'(\widetilde{t}) = \Delta x_{k-1}(\widetilde{t}) + \alpha\tau\Delta v_k(\widetilde{t}), \tag{2.7}$$

$$\Delta v_k(\widetilde{t}+\alpha\tau) = \Delta v_k(\widetilde{t}) + \alpha\tau\Delta v_k'(\widetilde{t}) = \Delta v_k(\widetilde{t}) + \alpha\tau\Delta a_k(\widetilde{t}), \tag{2.8}$$

where $\Delta a_k(\widetilde{t}) = a_{k+1}(\widetilde{t}) - a_k(\widetilde{t})$ represents the acceleration difference into the leading car $k+1$ and the following car k. Using eqs. (2.6) and (2.7), we can calculate the optimal velocities $V_F(\Delta x_k(\widetilde{t}+\alpha\tau))$ and $V_B(\Delta x_{k-1}(\widetilde{t}+\alpha\tau))$ as follow:

$$V_F(\Delta x_k(\widetilde{t}+\alpha\tau)) = V_F[\Delta x_k(\widetilde{t})] + V_F'[\Delta x_k(\widetilde{t})]\Delta v_k(\widetilde{t})\alpha\tau, \tag{2.9}$$

$$V_B(\Delta x_{k-1}(\widetilde{t}+\alpha\tau)) = V_B[\Delta x_{k-1}(\widetilde{t})] + V_B'[\Delta x_{k-1}(\widetilde{t})]\Delta v_{k-1}(\widetilde{t})\alpha\tau. \tag{2.10}$$

Using eqs. (2.8), (2.9) and (2.10) into eq. (2.5), we get

$$\begin{aligned}\frac{dv_k(\widetilde{t})}{d\widetilde{t}} &= \widetilde{a}[\omega V_F(\Delta x_k(\widetilde{t})) + (1-\omega)V_B(\Delta x_{k-1}(\widetilde{t})) - v_k(\widetilde{t})] + \alpha\omega V_F'(\Delta x_k(\widetilde{t}))\\ &\quad * \Delta v_k(\widetilde{t}) + \alpha(1-\omega)V_B'(\Delta x_{k-1}(\widetilde{t}))\Delta v_{k-1}(\widetilde{t}) + \lambda\Delta v_k(\widetilde{t}) + \lambda\alpha\tau\Delta a_k(\widetilde{t}).\end{aligned} \tag{2.11}$$

where $V_F'(\Delta x_k(\widetilde{t}))$ and $V_B'(\Delta x_{k-1}(\widetilde{t}))$ are the derivatives of forward and backward optimal velocity functions in form of headway respectively. The following are the optimal velocity functions:

$$\begin{aligned}V_F(\Delta x_k(\widetilde{t})) &= \frac{v_{\max}^F}{2}[\tanh(\Delta x_k(\widetilde{t}) - h_c) + \tanh(h_c)],\\ V_B(\Delta x_{k-1}(\widetilde{t})) &= -\frac{v_{\max}^B}{2}[\tanh(\Delta x_{k-1}(\widetilde{t}) - h_c) + \tanh(h_c)],\end{aligned} \tag{2.12}$$

where $v_{\max}^F$ is the forward maximum velocity, $v_{\max}^B$ is the backward maximum velocity and h_c is the safe distance. We take the value of ω from 0.5 to 1.0, as in driving, the value of forward concentration must be larger than backward concentration, $v_{\max}^F = v_{\max}^B = 2$ and $h_c = 4$.

3. Linear Stability Analysis

In this part, we investigate the effect of individual expectations and the BFL effect through linear stability analysis to understand the pattern of traffic congestion. Assume that traffic flow is stable at the beginning and that all cars N travel on a route of length L with a headway h and constant velocity $\omega V_F(h) + (1-\omega)V_B(h)$. As a result, the position of the car in the steady traffic flow is

$$x_k^0(\widetilde{t}) = hk + (\omega V_F(h) + (1-\omega)V_B(h))\widetilde{t}, \quad h = \frac{L}{N}. \tag{3.1}$$

From the traffic steady state $x_k^0(\widetilde{t})$, a small deviation $y_k(\widetilde{t}) = e^{(ijk+z\widetilde{t})}$ is made as

$$x_k(\widetilde{t}) = x_k^0(\widetilde{t}) + y_k(\widetilde{t}). \tag{3.2}$$

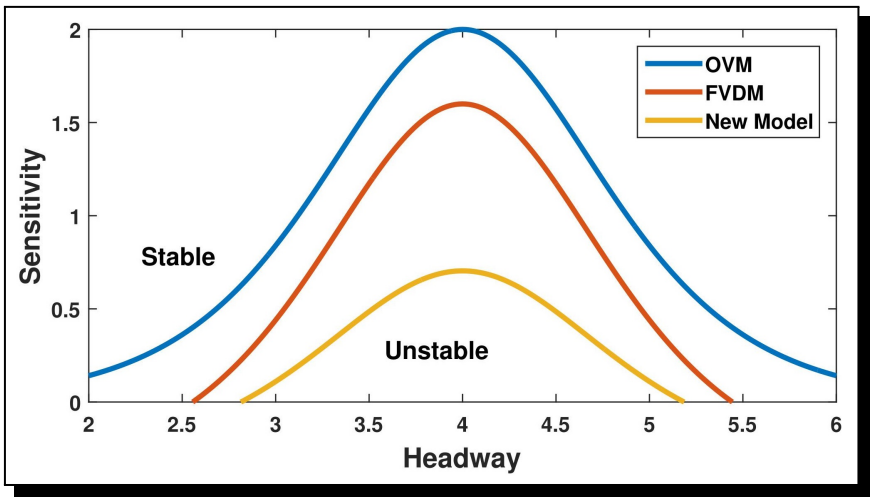

Figure 1. Phase diagram in parameter space (h,a) between OVM, FVDM and new model for fixed $\alpha = 0.2$, $\omega = 0.9$

Put eq. (3.2) into (2.11) and linearizing the derived equation, we get

$$\begin{aligned}\frac{d^2y_k(\widetilde{t})}{d\widetilde{t}^2} &= a\left[\omega V_F'(h)\Delta y_k(\widetilde{t}) + (1-\omega)V_B'(h)\Delta y_{(k-1)}(\widetilde{t}) - \frac{dy_k(\widetilde{t})}{d\widetilde{t}}\right] \\ &\quad + \alpha\omega V_F'(h)\left(\frac{dy_{k+1}(\widetilde{t})}{d\widetilde{t}} - \frac{dy_k(\widetilde{t})}{d\widetilde{t}}\right) + \alpha(1-\omega)V_B'(h)\left(\frac{dy_k(\widetilde{t})}{d\widetilde{t}} - \frac{dy_{k-1}(\widetilde{t})}{d\widetilde{t}}\right) \\ &\quad + \lambda\left(\frac{dy_{k+1}(\widetilde{t})}{d\widetilde{t}} - \frac{dy_k(\widetilde{t})}{d\widetilde{t}}\right) + \lambda\alpha\tau\left(\frac{d^2y_{k+1}(\widetilde{t})}{d\widetilde{t}^2} - \frac{d^2y_k(\widetilde{t})}{d\widetilde{t}^2}\right).\end{aligned} \tag{3.3}$$

Expanding $y_k(\widetilde{t})$ in eq. (3.3) by using Fourier series, we get

$$\begin{aligned}z^2 &= a[\omega V_F'(h)(e^{ij}-1) + (1-\omega)V_B'(h)(1-e^{-ij}) - z] + \alpha\omega V_F'(h)[z(e^{ij}-1)] \\ &\quad + \alpha(1-\omega)V_B'(h)[z(1-e^{-ij})] + \lambda z(e^{ij}-1) + \lambda\alpha\tau z^2(e^{ij}-1).\end{aligned} \tag{3.4}$$

Put $z = z_1(ij) + z_2(ij)^2 + \ldots$ and $e^{ij} = 1 + ij + \frac{1}{2}(ij)^2 + \ldots$, and ignoring term of order greater than 2 into eq. (3.4), we get

$$\begin{aligned}&[z_1(ij) + z_2(ij)^2 + \ldots]^2 \\ &= \widetilde{a}\left[\omega V_F'(h)\left(ij + \frac{(ij)^2}{2} + \ldots\right) + (1-\omega)V_B'(h)\left(ij - \frac{(ij)^2}{2} + \ldots\right) - (z_1(ij) + z_2(ij^2) + \ldots)\right] \\ &\quad + \alpha\omega V_F'(h)\left[(z_1(ij) + z_2(ij^2) + \ldots)\left(ij + \frac{(ij)^2}{2} + \ldots\right)\right] \\ &\quad + \alpha(1-\omega)V_B'(h)\left[(z_1(ij) + z_2(ij^2) + \ldots)\left(ij - \frac{(ij)^2}{2} + \ldots\right)\right] \\ &\quad + \lambda(z_1(ij) + z_2(ij^2) + \ldots)\left(ij + \frac{(ij)^2}{2} + \ldots\right) + \lambda\alpha\tau(z_1(ij) + z_2(ij^2) + \ldots)^2\left(ij + \frac{(ij)^2}{2} + \ldots\right).\end{aligned} \tag{3.5}$$

Equating, the first and second-order terms of ij, we obtain

$$z_1 = \omega V_F'(h) + (1-\omega)V_B'(h), \tag{3.6}$$

$$z_2 = \frac{\widetilde{a}(\omega V_F'(h) + (1-\omega)V_B'(h)) + 2(\alpha(\omega V_F'(h) + (1-\omega)V_B'(h)) + \lambda)z_1 - 2z_1^2}{2\widetilde{a}}. \tag{3.7}$$

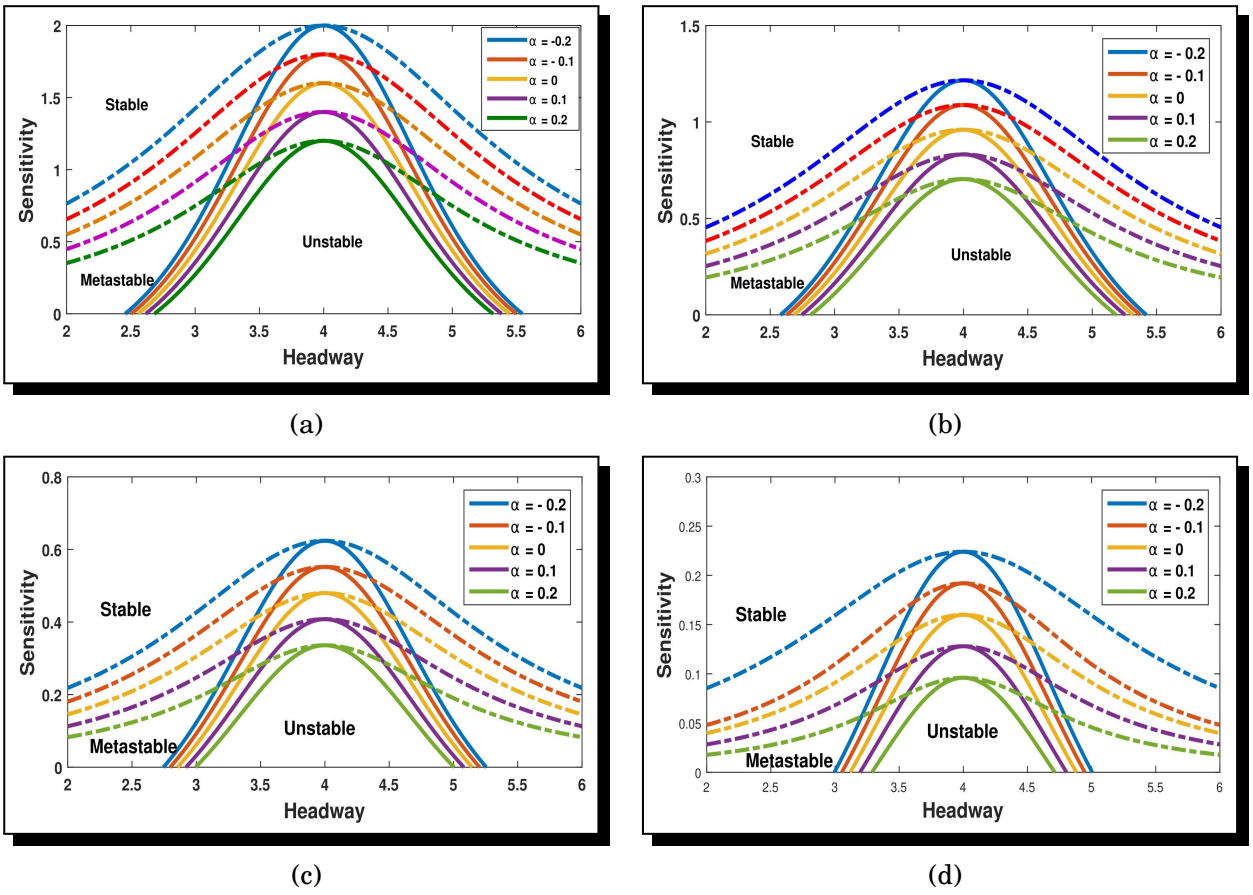

Figure 2. Phase diagram for the different α with fixed $\lambda = 0.2$ (a) $\omega = 1$, (b) $\omega = 0.9$, (c) $\omega = 0.8$, (d) $\omega = 0.7$

The condition of neutral stability is written as

$$\widetilde{a} = \frac{2(1-\alpha)(\omega V_F' + (1-\omega)V_B')^2 - 2\lambda(\omega V_F' + (1-\omega)V_B')}{(\omega V_F' + (1-\omega)V_B')}. \tag{3.8}$$

When a small perturbation with long wavelengths is applied to the uniform traffic flow, it becomes unstable.

$$\widetilde{a} < \frac{2(1-\alpha)(\omega V_F' + (1-\omega)V_B')^2 - 2\lambda(\omega V_F' + (1-\omega)V_B')}{(\omega V_F' + (1-\omega)V_B')}. \tag{3.9}$$

For $\alpha = 0$, the stability condition of the *Forward-Backward Velocity Difference Model* (FBVD) is obtained [14] as

$$\widetilde{a} < \frac{2(\omega V_F' + (1-\omega)V_B')^2 - 2\lambda(\omega V_F' + (1-\omega)V_B')}{(\omega V_F' + (1-\omega)V_B')}. \tag{3.10}$$

When $\alpha = 0$ and $\omega = 1$, the stability constraint of the *Full Velocity Difference Model* (FVDM) [16]

is as follows

$$\widetilde{a} < 2V'(h) - 2\lambda. \tag{3.11}$$

From eq. (3.9), we can conclude that the prediction parameter α and driver weight parameter ω, both have a substantial impact on traffic flow stabilization. Figure 1 shows the key similarity of the new, FVD, and OV models for fixed $\alpha = 0.2$ and $\omega = 0.9$ with $\lambda = 0.2$. On comparing the results of the OV and FVD models with a new model, it is obvious that the new model represents a more stable zone, revealing that the proposed model is an improvement over the existing literature.

In the parameter space $(h_c, \widetilde{a}_c)$, we replicate the neutral stability curves (solid lines) with coexisting curves (dotted lines) as depicted in Figure 2. The apex of the neutral stability line is denoted by the critical point and the zone of stability is located above the neutral curve, whereas traffic remains uniform when a small perturbation is added. The area below the neutral stability curve represents that the traffic is unstable, which means that it is affected by perturbation which converts into congestion with time. The amplitude of these curves diminishes as the value of the parameter α rises for fixed $\omega = 0.7, 0.8, 0.9, 1.0$ with fixed λ, as seen in Figures 2(a-d). The higher the value of α, the more stable the traffic flow is, effectively suppresses the traffic jam. For $\alpha < 0$ value, there is a physical delay in the vehicle motion, which induce traffic congestion, which can also be seen from Figuer 2.

Also seen in Figure 2, the stable region improves when the influence of previous sites is taken into account, and this effect becomes more effective when the effect of the driver's prediction parameter is taken into account. Consequently, the effect of the prediction parameter α and the BFL effect play an essential role in stabilizing traffic congestion.

4. Nonlinear Analysis

As we know that the nature of traffic systems is very complex, so linear analysis is not enough to accurately describe the real traffic state. Therefore, a nonlinear analysis is accomplished, to understand the nonlinear behavior of traffic flow in terms of the "kink-antikink" wave.

Equation (2.11) in form of headway can be rewritten as

$$\begin{aligned}
\frac{d^2\Delta x_k(\widetilde{t})}{d\widetilde{t}^2} = \widetilde{a}\Bigg[&\omega(V_F(\Delta x_{k+1}(\widetilde{t})) - V_F(\Delta x_k(\widetilde{t}))) + (1-\omega)(V_B(\Delta x_k(\widetilde{t})) - V_B(\Delta x_{k-1}(\widetilde{t}))) - \frac{d\Delta x_k(\widetilde{t})}{d\widetilde{t}}\Bigg] \\
&+ \alpha\omega(V_F'(\Delta x_{k+1}(\widetilde{t})) - V_F'(\Delta x_k(\widetilde{t})))\left(\frac{d\Delta x_k(\widetilde{t})}{d\widetilde{t}}\right) \\
&+ \alpha\omega(V_F'(\Delta x_k(\widetilde{t})))\left(\frac{d\Delta x_{k+1}(\widetilde{t})}{d\widetilde{t}} - \frac{d\Delta x_k(\widetilde{t})}{d\widetilde{t}}\right) \\
&+ \alpha(1-\omega)(V_B'(\Delta x_k(\widetilde{t})) - V_B'(\Delta x_{k-1}(\widetilde{t})))\left(\frac{d\Delta x_{k-1}(\widetilde{t})}{d\widetilde{t}}\right) \\
&+ \alpha(1-\omega)(V_B'(\Delta x_{k-1}(\widetilde{t})))\left(\frac{d\Delta x_k(\widetilde{t})}{d\widetilde{t}} - \frac{d\Delta x_{k-1}(\widetilde{t})}{d\widetilde{t}}\right) \\
&+ \lambda\left(\frac{d\Delta x_{k+1}(\widetilde{t})}{d\widetilde{t}} - \frac{d\Delta x_k(\widetilde{t})}{d\widetilde{t}}\right) + \lambda\alpha\tau\left(\frac{d^2\Delta x_{k+1}(\widetilde{t})}{d\widetilde{t}^2} - \frac{d^2\Delta x_k(\widetilde{t})}{d\widetilde{t}^2}\right).
\end{aligned} \tag{4.1}$$

Using the reductive perturbation method, we solve the eq. (4.1) by introducing a small-scale positive parameter ϵ near the critical point $(h_c, \widetilde{a}_c)$. The variables $\widetilde{t}$ and k have small scales, and are defined as

$$X = \epsilon(k + b\widetilde{t}),\ T = \epsilon^3\widetilde{t}, \quad 0 < \epsilon \le 1, \tag{4.2}$$

where the unspecified constant is b. The headway $\Delta x_k(\widetilde{t})$ is defined as

$$\Delta x_k(\widetilde{t}) = h_c + \epsilon R(X, T). \tag{4.3}$$

From eqs. (4.1), (4.2) and (4.3) and expanding using Taylor's series expansion up to the fifth power of ϵ, we get the following nonlinear evolution problem:

$$\begin{aligned}
&\epsilon^2(b - (\omega V_F' + (1-\omega)V_B')\partial_X R + \epsilon^3\left(\tau b^2 - \frac{1}{2}\left(\omega(V_F' + V_B') - V_B'\right) - \tau\alpha b(\omega V_F' + (1-\omega)V_B') - \lambda\tau b\right)\partial_X^2 R \\
&+ \epsilon^4\left[\partial_T R - \left(\frac{\omega V_F'}{6} - \frac{(1-\omega)V_B'}{6} + \frac{\tau\alpha b}{2}(\omega V_F' - (1-\omega)V_B') + \frac{\lambda\alpha b}{2} + \lambda\alpha\tau^2 b^2\right)\partial_X^3 R\right. \\
&\left. - \left(\frac{\omega V_F'''}{6} + \frac{(1-\omega)V_B'''}{6}\right)\partial_X R^3\right] \\
&+ \epsilon^5\left[-\left(\frac{\omega V_F'}{24} - \frac{(1-\omega)V_B'}{24} + \frac{\tau\alpha b}{6}(\omega V_F' - (1-\omega)V_B') + \frac{\lambda\alpha b}{6} + \frac{\lambda\alpha\tau^2 b^2}{2}\right)\partial_X^4 R\right] \\
&+ \epsilon^5\left[(2b\tau - \lambda\tau - \alpha\tau(\omega V_F' + (1-\omega)V_B'))\partial_X\partial_T R - \left(\frac{\omega V_F'''}{12} - \frac{(1-\omega)V_B'''}{12}\right)\partial_X^2 R^3\right] = 0,
\end{aligned} \tag{4.4}$$

where

$$\begin{aligned}
V_F' &= V_F'(h_c) = \frac{dV_F(\Delta x_k)}{d\Delta x_k}|_{\Delta x_k = h_c}, \quad V_B' = V_B'(h_c) = \frac{dV_B(\Delta x_{k-1})}{d\Delta x_{k-1}}|_{\Delta x_{k-1} = h_c}, \\
V_F''' &= V_F'''(h_c) = \frac{d^3V_F(\Delta x_k)}{d\Delta x_k^3}|_{\Delta x_k = h_c}, \quad V_B''' = V_B'''(h_c) = \frac{d^3V_B(\Delta x_{k-1})}{d\Delta x_{k-1}^3}|_{\Delta x_{k-1} = h_c}.
\end{aligned}$$

The traffic flow near the critical point $\tau = (1-\epsilon^2)\tau_c$, $\tau_c = \frac{\omega V_F' - (1-\omega)V_B'}{2b^2(1-\alpha) - 2\lambda b}$ and $b = \omega V_F' + (1-\omega)V_B'$ is introducing into eq. (4.4) and neglecting the terms of second and third orders of ϵ, we get

$$\epsilon^3(\partial_T R - q_1\partial_X^3 R + q_2\partial_X R^3) + \epsilon^5(q_3\partial_X^2 R + q_4\partial_X^4 R + q_5\partial_X^2 R^3) = 0, \tag{4.5}$$

where

$$\begin{aligned}
q_1 &= \frac{1}{6}b + \frac{1}{2}\lambda\tau_c b + \frac{1}{2}\tau_c\alpha b(\omega V_F' - (1-\omega)V_B') + \lambda\alpha\tau_c^2 b^2, \\
q_2 &= -\frac{1}{6}(\omega V_F''' + (1-\omega)V_B'''), \\
q_3 &= -b^2\tau_c + \lambda\tau_c b + \alpha\tau_c b^2, \\
q_4 &= (2\tau_c b - \lambda\tau_c - \alpha\tau_c b)\left(\frac{b}{6} + \frac{\tau_c\alpha b}{2}(\omega V_F' - (1-\omega)V_B') + \frac{\lambda\tau_c b}{2} + \lambda\alpha\tau_c^2 b^2\right) \\
&\quad - \left(\frac{\omega V_F'}{24} - \frac{(1-\omega)V_B'}{24} + \frac{\tau\alpha b^2}{6} + \frac{\lambda\tau b}{6} + \frac{\lambda\alpha\tau^2 b^2}{2}\right), \\
q_5 &= (2\tau_c b - \lambda\tau_c - \alpha\tau_c b)\left(\frac{\omega V_F''}{6} + \frac{(1-\omega)V_B''}{6}\right) - \frac{1}{12}(\omega V_F''' - (1-\omega)V_B''').
\end{aligned} \tag{4.6}$$

To obtained mKdV equation, the transformation (change of scale variable) is applied to eq. (4.5) as follows

$$T = \frac{1}{q_1}T', \quad R = \sqrt{\frac{q_1}{q_2}}R'. \tag{4.7}$$

Therefore, with such a $O(\epsilon)$ correction term, the conventional mKdV equation is given as:

$$\partial_{T'}R' = \partial_X^3 R' - \partial_X R'^3 - \epsilon\left(\frac{q_3}{q_1}\partial_X^2 R' + \frac{q_4}{q_1}\partial_X^4 R' + \frac{q_5}{q_1}\partial_X^2 R'^3\right). \tag{4.8}$$

The "kink-antikink" soliton is defined as in eq. (4.9), if the term $O(\epsilon)$ is neglected

$$R_0'(X,T') = \sqrt{c}\,\tanh\left[\sqrt{\frac{c}{2}}(X - cT')\right]. \tag{4.9}$$

The kink solution must meet the solvability requirement by $R_0'(X,T')$ and finding propagation velocity c:

$$(R_0', M[R_0']) \equiv \int_{-\infty}^{\infty} R_0' M[R_0']dX = 0, \tag{4.10}$$

where $M[R_0'] = \left(\frac{q_3}{q_1}\partial_X^2 R' + \frac{q_4}{q_1}\partial_X^4 R' + \frac{q_5}{q_1}\partial_X^2 R'^3\right)$.

With the help of the method described in [9], we get propagation velocity c as

$$c = \frac{5q_2q_3}{2q_2q_4 - 3q_1q_5}. \tag{4.11}$$

As a result, the generic kink-antikink solution is as follows:

$$\Delta x_k(t) = h_c \pm \sqrt{\frac{q_1 c}{q_2}\left(\frac{\tau}{\tau_c} - 1\right)} \times \left[(1 - cq_1)\left(\frac{\tau}{\tau_c} - 1\right)\widetilde{t} + k\right]. \tag{4.12}$$

The amplitude is

$$A = \sqrt{\frac{q_1 c}{q_2}\left(\frac{\tau}{\tau_c} - 1\right)}, \tag{4.13}$$

where $V_F''' < 0$, $V_B''' < 0$. The coexisting phase is defined by the general "kink-antikink" solution. The coexisting curves for the jammed and the free flow phase can be described by $\Delta x_k = h_c \pm A$. As a result, the mKdV equation can be used to characterize the jamming transition.

5. Numerical Simulation

To check the findings of the new model, the numerical simulation is performed with the closed boundary condition. We assume $N = 100$ is the total number of vehicles, $L = 400$ is the length of the road, $h = \frac{L}{N}$, $\lambda = 0.3$, $A = 1$ and the initial disturbances are chosen as follow:

$$\Delta x_k(0) = \Delta x_k(1) = \Delta x_k(2) = 4.0, \qquad (k \neq 50, 51),$$
$$\Delta x_k(0) = \Delta x_k(1) = \Delta x_k(2) = 4.0 + A, \quad (k = 50),$$
$$\Delta x_k(0) = \Delta x_k(1) = \Delta x_k(2) = 4.0 - A, \quad (k = 51).$$

In the simulation, we will investigate whether the initial disturbance increases or it is suppressed with time by the model's intrinsic stable dynamics in a deeper sense. For this, initially, we assumed that all vehicles are expected to have the same characteristics. In this study, we divide our results into two cases.

Case 1: No "Backward Looking" Effect

Here, we examine the impact of the prediction parameter on the traffic stability for $\omega = 1$, $a = 1.7s^{-1}$. Figure 3 represents the space-time evolution of the headway with different values of α between time 10000-10300s. For negative values of α, the initial perturbation evolves into a "kink-antikink" wave, which oscillates near the critical headway as shown in Figures 3(a-b).

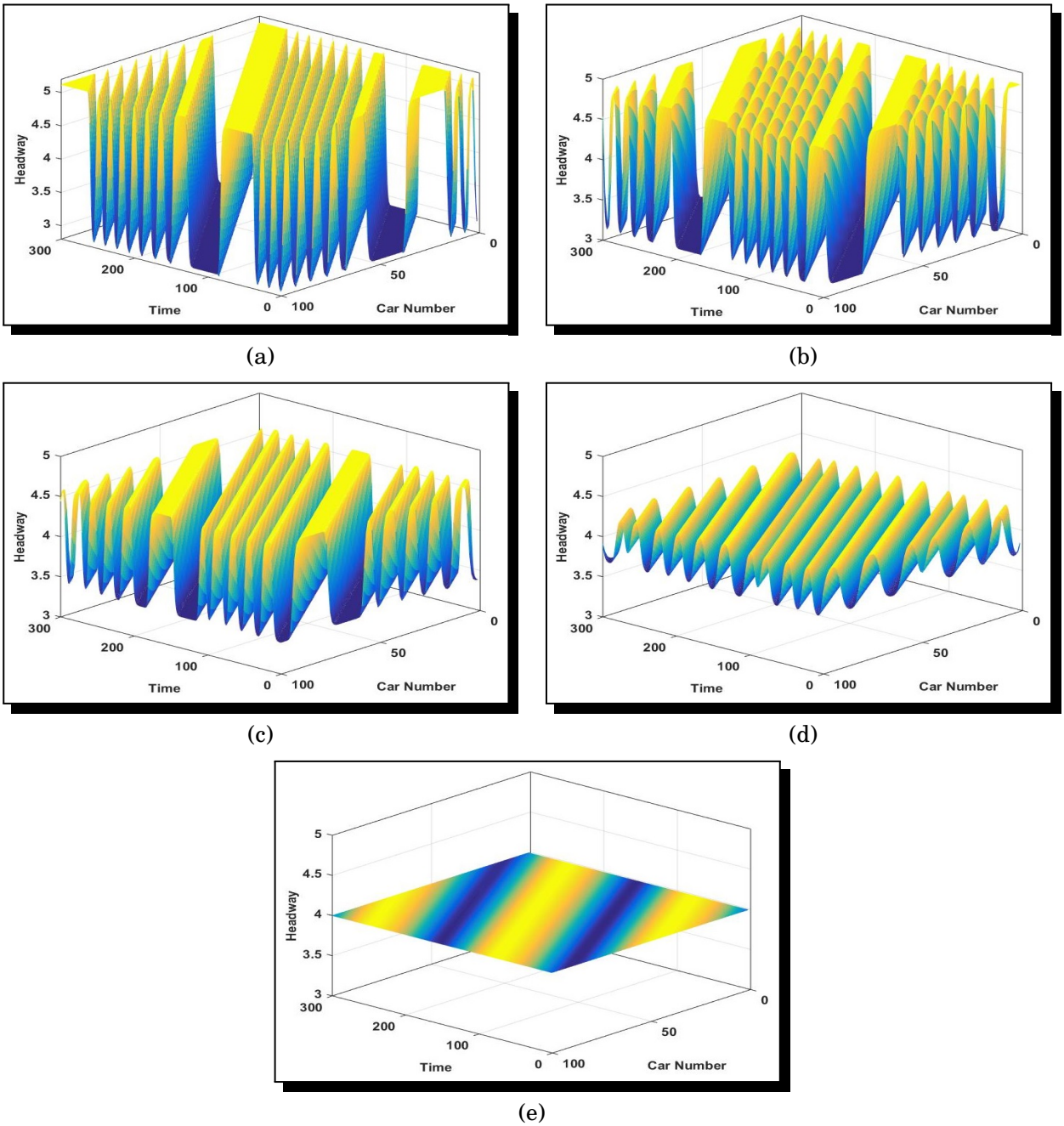

Figure 3. Space-time evolution of the headway with different parameter α at $\omega = 1$, (a) $\alpha = -0.2$, (b) $\alpha = -0.1$, (c) $\alpha = 0.0$, (d) $\alpha = 0.1$, (e) $\alpha = 0.2$

As we go from a negative to a positive value of α means delay to advance effect, the results corresponding to the decision of drivers can be easily seen from Figuers 3(c-e) that the number

of stop-and-go waves as well as their amplitude decreases with the increment in the value of α. Further, increase in the value of α, the disturbance dies out, and flow becomes stable for $\alpha = 0.2$. Figure 4 displays the headway profile for different values of prediction parameter α, for fixed $\omega = 1$ at $\widetilde{t} = 10300$ in respective of Figure 3 which indicates that amplitude of headway profile diminishes with α and flow become uniform for $\alpha = 0.2$. Therefore, the driver prediction parameter has a crucial role in alleviating congestion, as shown in Figures 3 and 4.

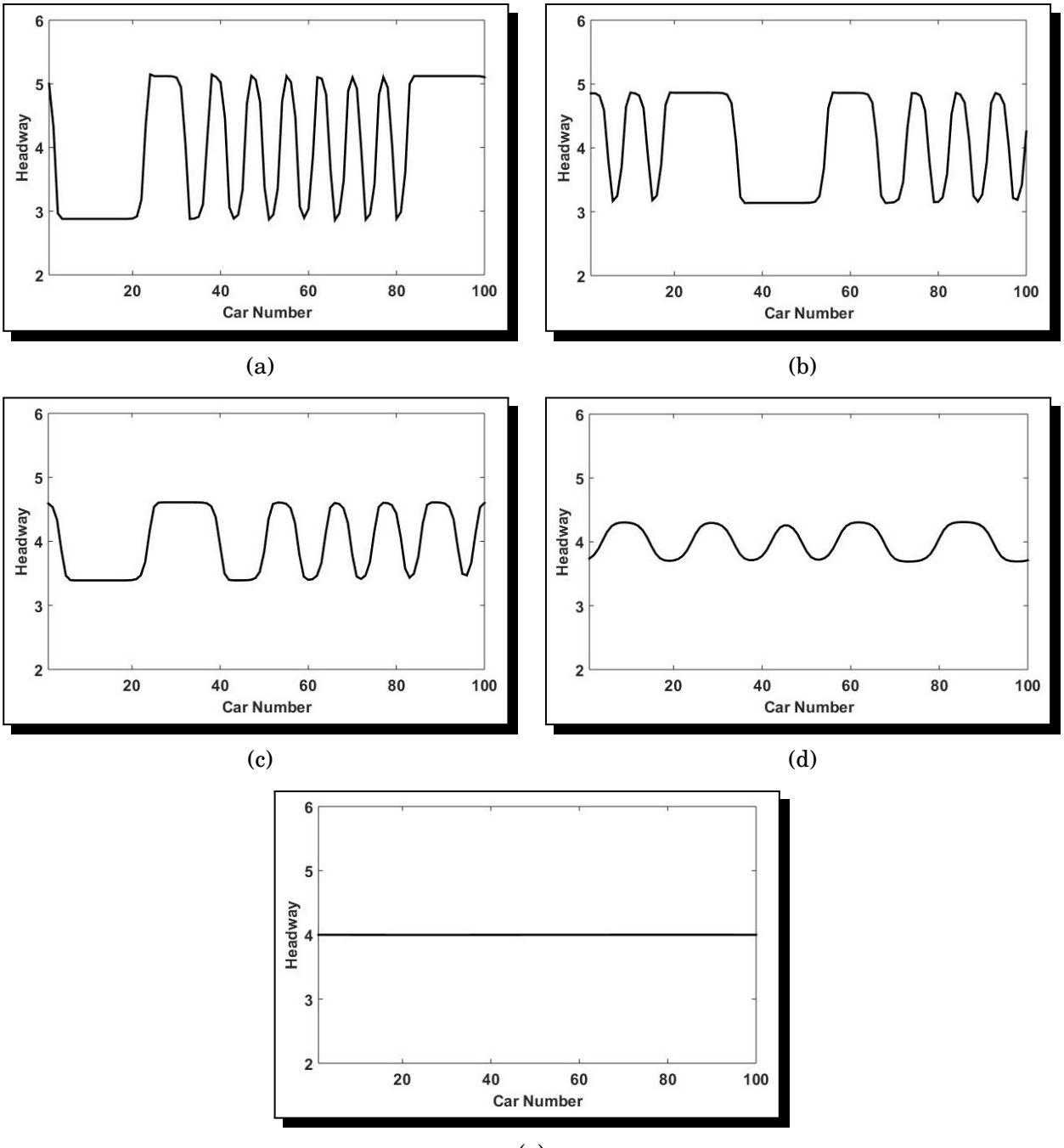

Figure 4. Snapshot of the headway at different values of α and fixed $\omega = 1$, (a) $\alpha = -0.2$, (b) $\alpha = -0.1$, (c) $\alpha = 0.0$, (d) $\alpha = 0.1$, (e) $\alpha = 0.2$

Case 2: With "Backward Looking" effect

Figure 5 shows that the space-time evolution of the headway with different values of α after $\widetilde{t} = 10000$, with fixed $\omega = 0.9$. As the stability condition is not satisfied for $-0.2 \leq \alpha \leq 0.1$, the initial perturbation evolves into congested flow in the form of kink waves which propagates in the backward direction and oscillates near the critical headway as shown in Figures 5(a-d). As we enter into the stable region for $\alpha = 0.2$, it is clear from Figure 5(e) that the congested flow converts into the uniform flow.

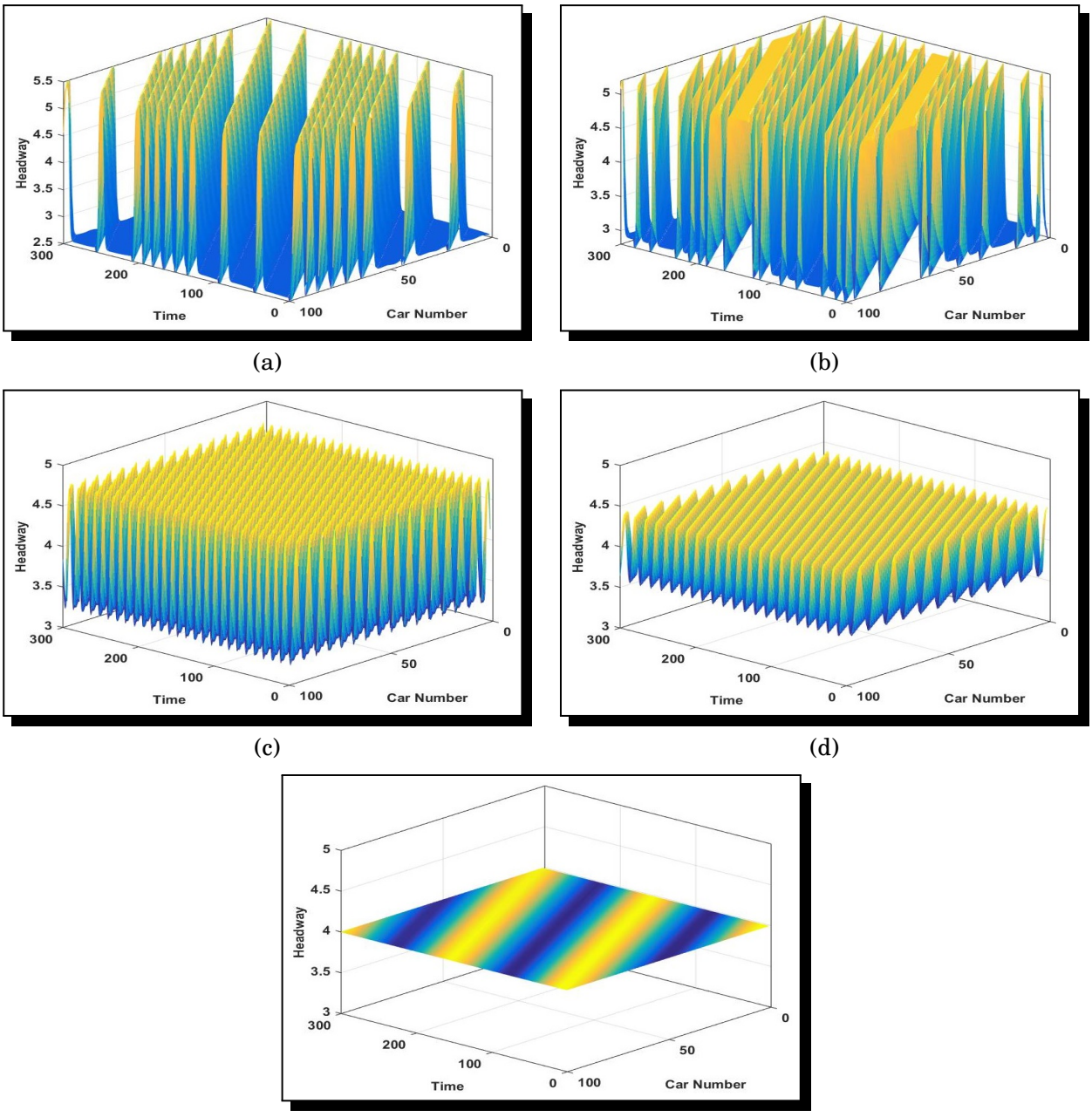

Figure 5. Space-time evolution of the headway with different parameter α at $\omega = 0.9$, (a) $\alpha = -0.2$, (b) $\alpha = -0.1$, (c) $\alpha = 0.0$, (d) $\alpha = 0.1$, (e) $\alpha = 0.2$

Figure 6 illustrates the headway profile for different values of prediction parameter α at $\widetilde{t} = 10300$ in respective of Figure 5. From Figure 6, it is concluded that the stable region is getting better with an increase in the value of α.

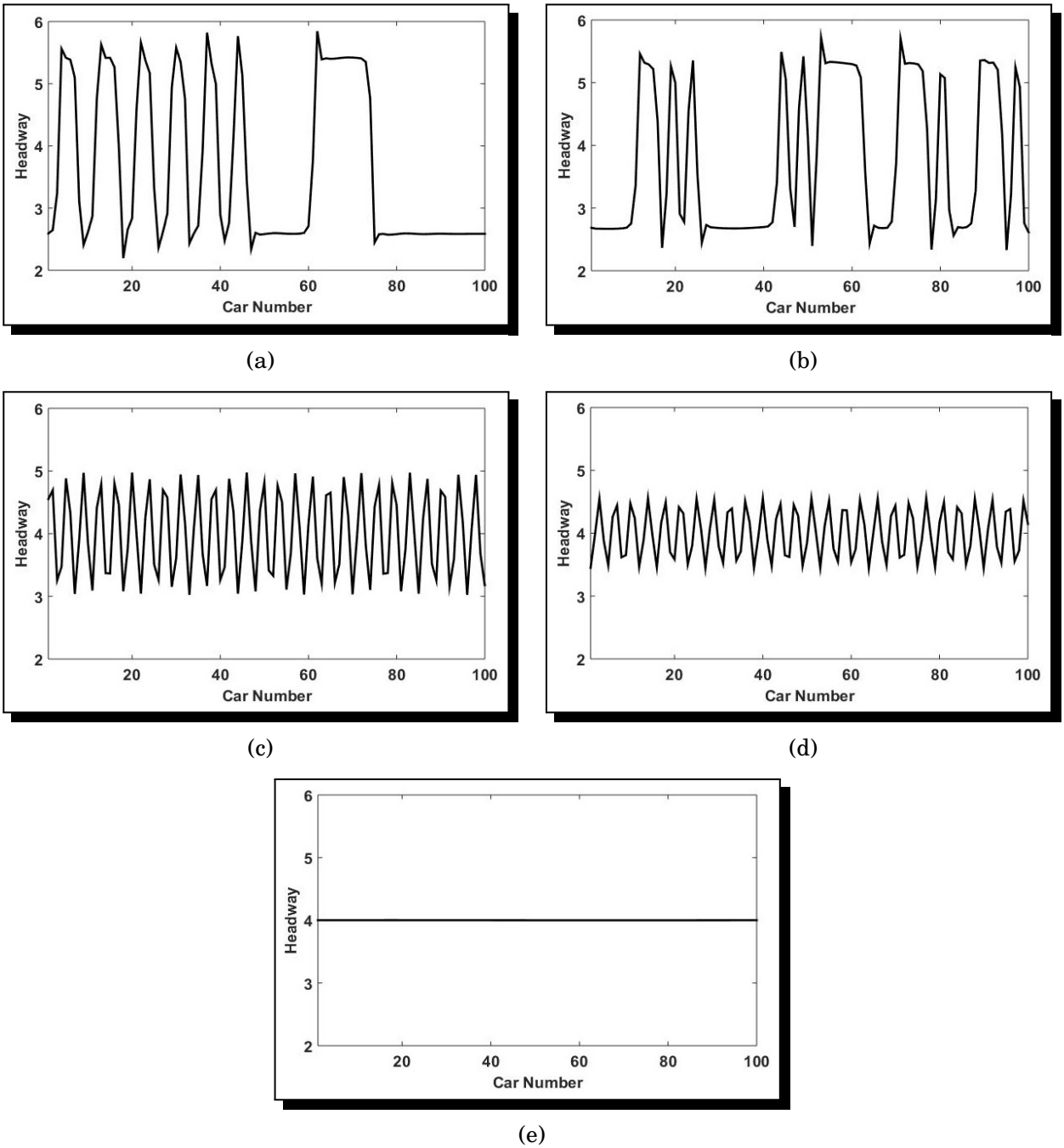

Figure 6. Snapshot of the headway at different values of α and fixed $\omega = 0.9$, (a) $\alpha = -0.2$, (b) $\alpha = -0.1$, (c) $\alpha = 0.0$, (d) $\alpha = 0.1$, (e) $\alpha = 0.2$

From Figures 4 and 6, it is clear that for positive values of α, the amplitude of these waves decreases with an increase in the value of α. On the other hand, for negative values of α, the amount of stop-and-go waves and also their amplitude increases with a decrease in the value of

the prediction effect. Therefore, it is obvious to say that the stable zone enhances with a rise in the value of α. This is because the significant delay introduced by human responses and mechanical control units ultimately generates external distractions in the whole dynamical system of traffic flow. On comparing the results of *Cases* 1 and 2, it is reasonable to conclude that the "backward-looking" effect further enhances the stability of traffic flow which is helpful in reducing external distractions.

6. Energy Consumption Control

As economic development and human consumption abilities grow, the energy usage of motorized vehicles has increased significantly for the general public. As a result, it is critical to figure out how to eliminate wasteful energy use in the transportation system. The energy consumption of the new model will be examined in this section. The kinetic energy theory states that vehicles use energy in order to work. According to the theorem, the velocity change of each vehicle at successive moments is investigated. The change in energy consumption is described as

$$\Delta E = \frac{1}{2}[v_k^2(\widetilde{t}) - v_k^2(\widetilde{t}-1)], \tag{6.1}$$

where $v_k^2(\widetilde{t})$ and $v_k^2(\widetilde{t}-1)$ is the velocity of vehicle k at two moments $(\widetilde{t}-1)$ and $\widetilde{t}$. In Figures 7 and 8, there are two zones with $\Delta E > 0$ indicates energy usage during movement, whereas $\Delta E < 0$ indicates energy usage during relaxation.

The fluctuation of energy consumption for different prediction parameters with fixed $\lambda = 0.3$ and $\omega = 1$ is shown in Figure 7. When the prediction parameter is increased, the amplitude variation of energy consumption decreases, indicating that the prediction effect can minimize kinetic transmission loss and hence reduce extra traffic energy usage.

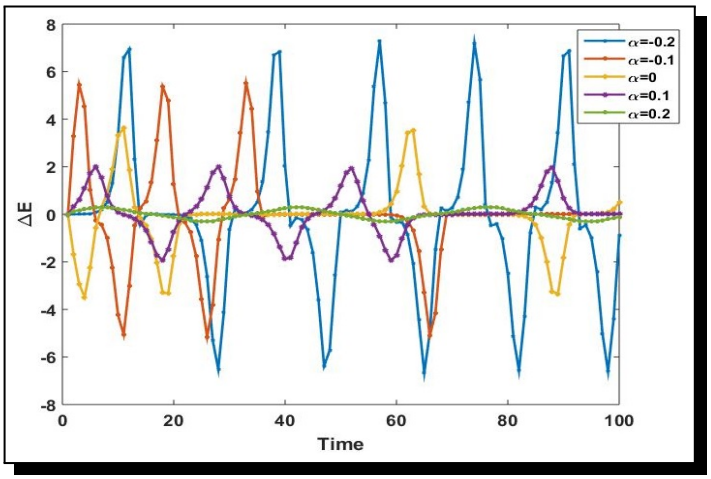

Figure 7. Energy consumption between the successive period of time for different values of α

The change in energy consumption for various parameters ω with fixed prediction parameter is depicted in Figuer 8. Figures 8(a) and 8(b) show that when the "backward-looking" impact is increased with a fixed prediction value, the energy consumption is reduced. It means that the by increasing the effect of the driver's prediction with the "backward-looking" effect reduces

energy consumption effectively. The results of the energy consumption are consistent with the headway of space-time evolution.

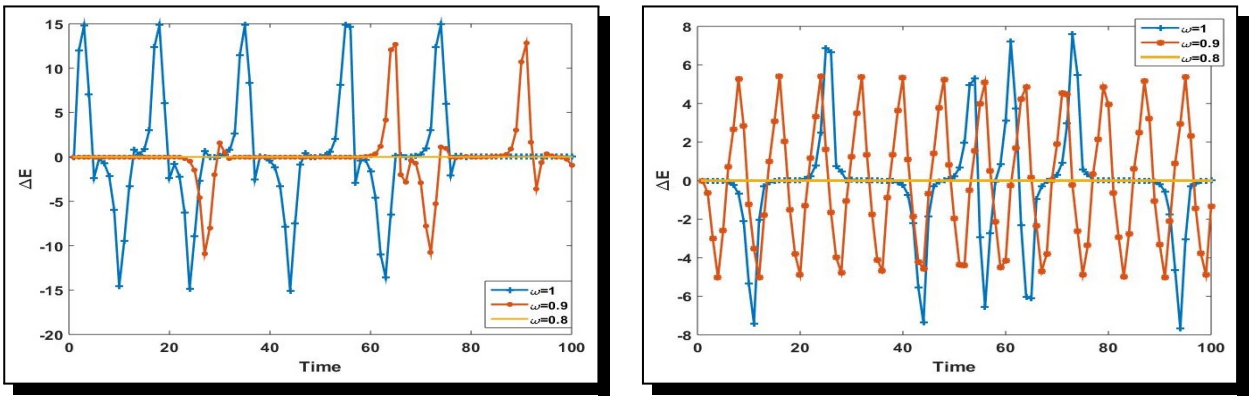

(a) (b)

Figure 8. Energy consumption successive period of time for different value of ω, (a) $\alpha = -0.2$, (b) $\alpha = 0.2$

Therefore, we noticed that the congestion may be reduced by including the contribution of preceding vehicles, and further, it can also be minimized if drivers make sensible decisions.

7. Conclusions

The effect of the driver's prediction is taken into consideration in a novel car-following model based on the BFL effect. Using linear and nonlinear analysis, the stability condition is derived near the critical point and nonlinear behavior is analyzed through the mKdV equation. From theoretical analysis, it is found that the stable region enhances with an increase in the value of the prediction parameter, and further enhances with an increase in the value of the backward effect. Furthermore, simulation findings are also confirmed with the theoretical analysis, demonstrating that the prediction parameter and BFL have a significant impact on traffic flow stability, which may be used to alleviate traffic congestion.

Through the study of energy consumption, it reveals that the proposed model can effectively fulfill the goals of reducing traffic instability and lowering energy consumption. As a result, it is appropriate to consider the driver prediction in traffic flow and its effect become prominent when the role of preceding sites is also considered.

Acknowledgment

The first author (Sunita) appreciates the "Council of Scientific and Industrial Research (CSIR), New Delhi, India" (File no. 09/382(0245)/2019-EMR-I) for the financial support to carry out this research work.

Competing Interests

The authors declare that they have no competing interests.

Authors' Contributions

All the authors contributed significantly in writing this article. The authors read and approved the final manuscript.

References

[1] M. Bando, K. Hasebe, A. Nakayama, A. Shibata and Y. Sugiyama, Dynamical model of traffic congestion and numerical simulation, *Physical Review E* **51**(2) (1995), 1035, DOI: 10.1103/PhysRevE.51.1035.

[2] M. Bando, K. Hasebe, A. Nakayama, A. Shibata and Y. Sugiyama, Structure stability of congestion in traffic dynamics, *Japan Journal of Industrial and Applied Mathematics* **11**(2) (1994), 203 – 223, DOI: 10.1007/BF03167222.

[3] P. Berg, A. Mason and A. Woods, Continuum approach to car-following models, *Physical Review E* **61**(2) (2000), 1056 – 1066, DOI: DOI: 10.1103/PhysRevE.61.1056.

[4] R. E. Chandler, R. Herman and E. W. Montroll, Traffic dynamics: Studies in car following, *Operations Research* **6**(2) (1958), 165 – 184, URL: https://www.jstor.org/stable/167610.

[5] A. Ferrara, S. Sacone and S. Siri, Microscopic and mesoscopic traffic models, in: *Freeway Traffic Modelling and Control*, Advances in Industrial Control series, Springer, Cham., 113 – 143 (2018), DOI: 10.1007/978-3-319-75961-6_5.

[6] D. C. Gazis, R. Herman and R. B. Potts, Car-following theory of steady-state traffic flow, *Operations Research* **7**(4) (1959), 499 – 505, URL: https://www.jstor.org/stable/166948.

[7] H.-X. Ge and R.-J. Cheng, The "backward looking" effect in the lattice hydrodynamic model, *Physica A: Statistical Mechanics and its Applications* **387**(28) (2008), 6952 – 6958, DOI: 10.1016/j.physa.2008.05.060.

[8] H. X. Ge, R. J. Cheng and Z. P. Li, Two velocity difference model for a car following theory, *Physica A: Statistical Mechanics and its Applications* **387**(21) (2008), 5239 – 5245, DOI: 10.1016/j.physa.2008.02.081.

[9] H. X. Ge, R. J. Cheng and S. Q. Dai, KdV and kink–antikink solitons in car-following models, *Physica A: Statistical Mechanics and its Applications* **357**(3-4) (2005), 466 – 476, DOI: 10.1016/j.physa.2005.03.059.

[10] A. K. Gupta and P. Redhu, Analyses of the driver's anticipation effect in a new lattice hydrodynamic traffic flow model with passing, *Nonlinear Dynamics* **76**(2) (2014), 1001 – 1011, DOI: 10.1007/s11071-013-1183-2.

[11] D. Helbing and B. Tilch, Generalized force model of traffic dynamics, *Physical Review E* **58**(1) (1998), 133, DOI: 10.1103/PhysRevE.58.133.

[12] R. Herman, E. W. Montroll, R. B. Potts and R. W. Rothery, Traffic dynamics: Analysis of stability in car following, *Operations Research* **7**(1) (1959), 86 – 106, URL: https://www.jstor.org/stable/167596.

[13] S. P. Hoogendoorn and P. H. L. Bovy, Generic gas-kinetic traffic systems modeling with applications to vehicular traffic flow, *Transportation Research Part B: Methodological* **35**(4) (2001), 317 – 336, DOI: 10.1016/S0191-2615(99)00053-3.

[14] M. A. Hossain, K. M. A. Kabir and J. Tanimoto, Improved car-following model considering modified backward optimal velocity and velocity difference with backward-looking effect, *Journal of Applied Mathematics and Physics* **9**(2) (2021), 242 – 259, DOI: 10.4236/jamp.2021.92018.

[15] A. Jafaripournimchahi, L. Sun and W. Hu, Driver's anticipation and memory driving car-following model, *Journal of Advanced Transportation* **2020** (2020), Article ID 4343658, DOI: 10.1155/2020/4343658.

[16] R. Jiang, Q. Wu and Z. Zhu, Full velocity difference model for a car-following theory, *Physical Review E* **64**(1) (2001), 017101, DOI: 10.1103/PhysRevE.64.017101.

[17] Z. Jin, Z. Yang and H. Ge, Energy consumption investigation for a new car-following model considering driver's memory and average speed of the vehicles, *Physica A: Statistical Mechanics and its Applications* **506** (2018), 1038 – 1049, DOI: 10.1016/j.physa.2018.05.034.

[18] Y.-C. He, G. Zhang and D. Chen, Effect of density integration on the stability of a new lattice hydrodynamic model, *International Journal of Modern Physics B* **33**(9) (2019), 1950071, DOI: 10.1142/S0217979219500711.

[19] Y. Li, L. Zhang, H. Zheng, X. He, S. Peeta, T. Zheng and Y. Li, Evaluating the energy consumption of electric vehicles based on car-following model under non-lane discipline, *Nonlinear Dynamics* **82**(1) (2015), 629 – 641, DOI: 10.1007/s11071-015-2183-1.

[20] J. Li, Q.-Y. Chen, H. Wang and D. Ni, Analysis of LWR model with fundamental diagram subject to uncertainties, *Transportmetrica* **8**(6) (2012), 387 – 405, DOI: 10.1080/18128602.2010.521532.

[21] G. Ma, M. Ma, S. Liang, Y. Wang and H. Guo, Nonlinear analysis of the car-following model considering headway changes with memory and backward looking effect, *Physica A: Statistical Mechanics and its Applications* **562** (2021), 125303, DOI: 10.1016/j.physa.2020.125303.

[22] G. Ma, M. Ma, S. Liang, Y. Wang and Y. Zhang, An improved car-following model accounting for the time-delayed velocity difference and backward looking effect, *Communications in Nonlinear Science and Numerical Simulation* **85** (2020), 105221, DOI: 10.1016/j.cnsns.2020.105221.

[23] T. Nagatani, The physics of traffic jams, *Reports on Progress in Physics* **65**(9) (2002), 1331, DOI: 10.1088/0034-4885/65/9/203.

[24] A. Nakayama, Y. Sugiyama and K. Hasebe, Effect of looking at the car that follows in an optimal velocity model of traffic flow, *Physical Review E* **65**(1) (2001), 016112, DOI: 10.1103/PhysRevE.65.016112.

[25] D. Ngoduy, Application of gas-kinetic theory to modelling mixed traffic of manual and ACC vehicle, *Transportmetrica* **8**(1) (2012), 43 – 60, DOI: 10.1080/18128600903578843.

[26] G. H. Peng, A study of wide moving jams in a new lattice model of traffic flow with the consideration of the driver anticipation effect and numerical simulation, *Physica A: Statistical Mechanics and its Applications* **391**(23) (2012), 5971 – 5977, DOI: 10.1016/j.physa.2012.07.039.

[27] G. H. Peng and R.-J. Cheng, A new car-following model with the consideration of anticipation optimal velocity, *Physica A: Statistical Mechanics and its Applications* **392**(17) (2013), 3563 – 3569, DOI: 10.1016/j.physa.2013.04.011.

[28] G. H. Peng, W. Song, Y. J. Peng and S. H. Wang, A novel macro model of traffic flow with the consideration of anticipation optimal velocity, *Physica A: Statistical Mechanics and its Applications* **398** (2014), 76 – 82, DOI: 10.1016/j.physa.2013.12.015.

[29] P. Redhu and A. K. Gupta, Delayed-feedback control in a Lattice hydrodynamic model, *Communications in Nonlinear Science and Numerical Simulation* **27**(1-3) (2015), 263 – 270, DOI: 10.1016/j.cnsns.2015.03.015.

[30] C. Rongjun, G. Hongxia and W. Jufeng, The nonlinear analysis for a new continuum model considering anticipation and traffic jerk effect, *Applied Mathematics and Computation* **332** (2018), 493 – 505, DOI: 10.1016/j.amc.2018.03.077.

[31] Y. Sun, H. Ge and R. Cheng, An extended car-following model under V2V communication environment and its delayed-feedback control, *Physica A: Statistical Mechanics and its Applications* **508** (2018), 349 – 358, DOI: 10.1016/j.physa.2018.05.102.

[32] D.-H. Sun, X.-Y. Liao and G.-H. Peng, Effect of looking backward on traffic flow in an extended multiple car-following model, *Physica A: Statistical Mechanics and its Applications* **390**(4) (2011), 631 – 635, DOI: 10.1016/j.physa.2010.10.016.

[33] T. Q. Tang, C. Y. Li and H. J. Huang, A new car-following model with the consideration of the driver's forecast effect, *Physics Letters A* **374**(38) (2010), 3951 – 3956, DOI: 10.1016/j.physleta.2010.07.062.

[34] T. Q. Tang, H. J. Huang, S. G. Zhao and G. Xu, An extended ov model with consideration of driver's memory, *International Journal of Modern Physics B* **23**(05) (2009), 743 – 752, DOI: 10.1142/S0217979209051966.

[35] T.-Q. Tang, J. He, S.-C. Yang and H.-Y. Shang, A car-following model accounting for the driver's attribution, *Physica A: Statistical Mechanics and its Applications* **413** (2014), 583 – 591, DOI: 10.1016/j.physa.2014.07.035.

[36] A. K. Verma, A. K. Gupta and I. Dhiman, Phase diagrams of three-lane asymmetrically coupled exclusion process with Langmuir kinetics, *Europhysics Letters* **112**(3) (2015), 30008, DOI: 10.1209/0295-5075/112/30008.

[37] S. Wei and X. Yu, Study on stability and energy consumption in typical car-following models, *Physica A: Statistical Mechanics and its Applications 381* (2007), 399 – 406, DOI: 10.1016/j.physa.2007.02.106.

[38] K. Yi-Rong, S. Di-Hua and Y. Shu-Hong, A new car-following model considering driver's individual anticipation behavior, *Nonlinear Dynamics* **82** (2015), 1293 – 1302, DOI: 10.1007/s11071-015-2236-5.

[39] R. Zhang and E. Yao, Mesoscopic model framework for estimating electric vehicles' energy consumption, *Sustainable Cities and Society* **47** (2019), 101478, DOI: 10.1016/j.scs.2019.101478.

[40] G. Zhang, The self-stabilization effect of lattice's historical flow in a new lattice hydrodynamic model, *Nonlinear Dynamics* **91**(2) (2018), 809 – 817, DOI: 10.1007/s11071-017-3911-5.

[41] X. Zhao and Z. Gao, A new car-following model: full velocity and acceleration difference model, *The European Physical Journal B – Condensed Matter and Complex Systems* **47**(1) (2005), 145 – 150, DOI: 10.1140/epjb/e2005-00304-3.

[42] L.-J. Zheng, C. Tian, D.-H. Sun and W.-N. Liu, A new car-following model with consideration of anticipation driving behavior, *Nonlinear Dynamics* **70**(2) (2012), 1205 – 1211, DOI: 10.1007/s11071-012-0524-x.

[43] W.-X. Zhu and H. M. Zhang, Analysis of mixed traffic flow with human-driving and autonomous cars based on car-following model, *Physica A: Statistical Mechanics and its Applications* **496** (2018), 274 – 285, DOI: 10.1016/j.physa.2017.12.103.